Analysis of Heavy-Ion Beam Images and Comparison to Retarding Potential Analyzer Measurements

Beth Ellen Rosenberg

University of California, Berkeley

Lawrence Berkeley National Laboratory

Berkeley, California

August 10, 2005

Prepared in partial fulfillment of the requirements of the Office of Science, Department of Energy's Science Undergraduate Laboratory Internship under the direction of Peter Seidl in the Accelerator and Fusion Research Division at Lawrence Berkeley National Laboratory.

Participant: _____
Signature

Research Advisor: _____
Signature

Table of Contents

Abstract

Analysis of Heavy-Ion Beam Images and Comparison to Retarding Potential Analyzer Measurements. BETH ELLEN ROSENBERG (University of California, Berkeley; Berkeley, CA 94720), PETER SEIDL (Lawrence Berkeley National Laboratory, Berkeley, California 94720), ART MOLVIK (Lawrence Livermore National Laboratory, Livermore, California 94550), MICHEL KIREEFF COVO (UC Berkeley and LLNL)

It has been predicted that world energy demand will soon put enormous pressure on the currently available energy sources. Fusion energy is a potential solution to this problem if it can be controlled and converted into electricity in an economically feasible manner. One type of potential fusion energy plant uses heavy-ion beam drivers for inertial fusion energy. As part of the High Current Experiment (HCX), we seek to understand the injection, transport and focusing of high-current ion beams, by investigating the interactions of background gas and electrons (which can deteriorate the beam quality) with the primary K^+ beam. We present here a method of analyzing the electrostatic potential distribution due to the beam space charge within the grounded conducting vacuum pipe. This method enables tracking of ions arising from the ionization of background gas atoms by the incident K^+ beam. The beam intensity distribution is obtained from images gathered using a scintillator placed in the beam path. These data are used to calculate the expelled ion energy distribution, which is then compared to data collected from a Retarding Potential Analyzer (RPA). The comparison of the image analysis with RPA measurements is in fair agreement, given model and experimental uncertainties. Some remaining issues to be explored include the apparent correlation of maximum beam potential with RMS beam size, the systematic effect of background subtraction in the images, as well as possible 3D effects. The new method offers an improved capability to investigate and understand the physics

of intense beams, furthering the development of a viable heavy-ion driver for an inertial fusion power plant, which is intended to make fusion energy an affordable and environmentally attractive source of electric power.

Introduction

Many sources predict that in the next twenty to fifty years, the world will begin running out of fossil fuels [1]. Presently, a number of options exist for creating electricity; however, each of those alternatives has their own environmental drawbacks. A notable exception is fusion power. If it can be generated in an economically feasible manner, fusion energy promises to be a clean and abundant source of electrical power. Unlike fossil fuels, it does not create greenhouse gases, and unlike fission, it does not create long-lived radioactive waste. Fusion is a reaction in which two light atomic nuclei, such as deuterium and tritium, combine, or fuse, to become a single heavier nucleus (figure 1). Deuterium (^{2}H) and tritium (^{3}H), are easily obtained; deuterium is readily available from water, and tritium can be created from the fusion process itself. Currently, the most pressing obstacle to reliable fusion power is the exceptionally high temperature, more than 100 million degrees, required to initiate and sustain the reaction [2].

Two methods of creating and controlling the extreme temperatures of fusion energy are presently being investigated: inertial confinement fusion and magnetic confinement fusion. Both of these techniques are designed to keep the nuclear fuel from contact with the materials surrounding them, as such contact would immediately cool the fuel below a temperature where it can burn. Inertial confinement fusion employs inertia to contain and pressurize a small, bb-sized fuel pellet as it is heated and undergoes fusion (figure 2). In order to maintain confinement, the fuel pellet must be brought to fusion ignition temperature (~10 keV) within ten nanoseconds. In order to attain the required heat within the permissible time, the fuel pellet must be bombarded with energy at a rate near 400 Terawatts, or 4×10^{14} J/s [3]. The methods presently being investigated to supply this intense amount of power are laser and heavy-ion beam drivers. Heavy-ion drivers have been identified as the more promising means to produce electricity for

commercial use, as they are currently better able to handle the high repetition rates required to supply viable amounts of electrical power, as well as being more efficient and reliable for long-term use [2].

As part of the High Current Experiment (HCX), we seek to understand the injection, transport and focusing of high-current ion beams by conducting experiments with driver scale beams, complemented by numerical simulation. The current focus is on gathering and analyzing data related to the accumulation of electrons and their effect on beam quality during transport. Here we present a new method of estimating the equipotential lines within an ion beam. This method enables tracking of individual particles within the beam and reveals information regarding the energy and quantity of gas ions expelled by the beam. The beam intensity for each point in the beam pipe is obtained from images gathered using a scintillator placed in the beam path. These data are used to construct equipotentials, which are then correlated and confirmed with data collected from a Retarding Potential Analyzer (RPA). Knowledge of the equipotentials within the beam improves understanding of the gas and electron interactions with the beam that deteriorate the beam quality, and thus detract from beam control and focus. The method allows increased understanding of the physics of intense beams, furthering the development of a viable heavy-ion driver for an inertial fusion power plant, which is intended to make fusion energy an affordable and environmentally attractive source of electric power.

Materials and Methods

High Current Experiment

The HCX heavy-ion beam, consisting of 1 MeV singly-charged potassium ions, was generated using a K^+ ion source and injector. The beam was then passed through the matching

section, consisting of six electrostatic quadrupoles, where it was compressed to produce the matched beam parameters for transport. The electrostatic transport section is comprised of ten electrostatic quadrupole lenses. The last section of the HCX consists of 4 pulsed magnetic quadrupoles; it is between the third and fourth of these that the scintillator was placed [4]. A diagnostic section at the end of the beam line includes a Faraday Cup to measure the beam current (figure 3). The beam pulse duration is 5.0 μs, with the ions traveling at a speed of 2.2 m/μs, giving a beam length of 11 m.

The scintillator (figure 4) is used to create a photographic image of the beam (figure 5), with pixel intensity corresponding to the charge concentration of beam particles striking the scintillator. During these runs, the scintillator plate was placed in the beam path and a gated, image-intensified CCD camera was placed at the location of the Faraday Cup.

Image Analysis

The data were first processed through IMAGEJ [5], and then analyzed with routines written in MATLAB^{TM}. The routines were used to perform all manipulations of the data, including background subtraction and intensity calculations. Beam current data was collected with the Faraday cup and integrated over time slices equivalent to that of each scintillator image, to describe the total charge represented in each image. The charge was then related to the image intensity through a conversion factor to determine the relative charge per image pixel; the conversion factor was calculated individually for each image. Figure 6 shows the correspondence between charge and total intensity. Using the calculated charge density, the beam equipotentials were found, using the method of image charges for a cylinder of constant voltage, and the equation for the potential of a uniform line charge (figure 7). This method allowed for the

voltage at the radial distance of 4 cm from the center of the beam pipe to be set equal to zero, to fit the average dimensions of the beam pipe. The charge density was also used, in connection with cross section data, to predict the number of background gas ions expelled from each pixel. The expelled ion concentration and trajectories predicted with a MATLAB^{TM} routine enabled calculation of the number of expelled ions per unit energy interval that would enter the region of the RPA (figure 8) when it is installed, in place of the scintillator. This data was then compared with the data collected in previous experiments with the RPA.

Results

Voltage Calculation

The data under investigation comprises 12 scintillator images, representing one beam pulse. The time slice represented by the first three images was 0.25 μs; the rest of the images comprise 0.5 μs. The accuracy of the time placement for the first three images and last image relative to the rapidly evolving beam distribution at the head and tail of the beam pulse was insufficient and we chose to omit these from subsequent analysis described here. Figure 9 displays the good correspondence between the charge distribution captured in the scintillator images, and that predicted in simulations initialized with optical data gathered upstream of the scintillator. Regarding background subtraction issues, Fig. 10 shows that there is significant noise in the images, at the edge of the beam pipe location; this "halo" is ~25% of the peak beam intensity. The noise was determined to be reflection from the beam pipe and was removed from the calculations. Figure 11 shows the voltage distribution for a sample time slice, at a background cutoff of 90 (in units of intensity); the distribution shape is similar with small variations in all of the time slices under consideration. The upper limit of voltage in each image was found to be sensitive (~15%) to the background cutoff. Table 1 shows the maximum voltage

for all of the time slices under consideration at a cutoff of 200. The variation between images with constant background cutoff is on the order of (10%). Table 2 shows the effect of varying cutoff over five time slices; 90 being the minimum background pixel intensity in the area under consideration, and 200 being 10% of the maximum pixel intensity of the beam. The same variation in voltage between images was found at each cutoff. Various tests were run to determine what might be the cause of these variations. Figure 12 shows an inverse correlation between the voltage and beam size. Figure 13 shows the relationship between the voltage and the centroid position relative to the center of the beam pipe.

RPA Comparison

A single image was selected as a representative voltage distribution and used for comparison with data from the RPA. In order to compare the voltage data gathered from the scintillator images with that from the Retarding Potential Analyzer, it was necessary to find the number of background gas particles per voltage increment that would enter the RPA. The data available for comparison was that of nitrogen background gas, with an ionization cross-section of $6x10^{-16}$ cm^2, and a nitrogen pressure of $6x10^{-7}$ Torr ($1.98x10^{15}$ m^{-3}). The starting locations and voltages of relevant particles were determined using the dimensions of the RPA and trajectories predicted by placing test particles at each pixel location in a voltage matrix (Figure 14). The comparison of data gathered from the RPA, and that predicted using the scintillator image is shown in Fig. 15.

Discussion and Conclusions

The peak voltages shown in Table 1 vary between time-slices more than expected. Results from simulations, as well as the RPA had predicted or measured a relatively constant, or

even decreasing, peak voltage. Investigation into the cause of disparity has not yet been completed. The correlation between peak voltage and centroid motion shown in figure 13 was determined to be incidental; relocating the centroid with respect to the center of the beam pipe caused little change in the resulting voltage. The strong inverse correlation between peak voltage and RMS beam width shown in figure 12 is being investigated, and appears promising for revealing the cause of the disparity between measured and calculated peak voltages. Once the disparity is understood and normalized, the proper background cutoff for use in further experiments and analyses shall be determined based, in part, on Table 2. The effect of variations in background cutoff on peak voltages displayed in Table 2 implies changes in the potentials at the ≈5% level, large enough to require further consideration.

Figure 15 demonstrates that the shape of the energy distribution predicted using the scintillator data is in fair agreement with the RPA measurements. The disparities in height and shape between the RPA and scintillator data may be due to the fact that the distribution of the background gas during beam flight is not uniform or static; there is some evidence of desorbed gases entering the area of the beam. The question is whether the desorbed gas velocity distribution has a fast enough component so that gas atoms would cross the beam path before the entire beam has left the region of the RPA. Figure 15 also contains information regarding the effect of varying the background cutoff. While the higher cutoff produces higher voltages, which are closer to the RPA measurements, there is some loss of significant data, including that of the beam halo. The cutoff will have to be determined carefully for future experiments, based on the desired sensitivity. After this has been done, the data can be normalized to account for the cutoff's effect on voltage.

The comparison with RPA measurements shows that the methods for calculating beam potential distribution and predicting particle trajectories work reliably. The method and techniques still require fine-tuning, and further runs need to be made to verify and improve the results.

Acknowledgements

This research was conducted at the Lawrence Berkeley National Laboratory. I thank the U.S Department of Energy, Office of Science for giving me the opportunity to participate in the SULI program and the chance to participate in this research. Special thanks go to my mentor, Peter Seidl, as well as Art Molvik, and Michel Kireeff Covo, for their guidance and support.

References

[1] Paul B. Weisz, "Basic Choices and Constraints on Long-Term Energy Supplies", available: http://www.aip.org/pt/vol-57/iss-7/p47.html

[2] "Tutorial on Heavy-Ion Fusion Energy" [online document] Available: http://hif.lbl.gov/tutorial/tutorial.html

[3] "NIF Facts" [online document] Available: http://www.llnl.gov/nif/project/lib_presskit.html

[4] L. R. Prost, P. A. Seidl, F. M. Bieniosek, C. M. Celata, A. Faltens, D. Baca, E. Henestroza, J. W. Kwan, M. Leitner, W. L. Waldron, R. Cohen, A. Friedman, D. Grote, S. M. Lund, A. W. Molvik, and E. Morse, "High current transport experiment for heavy ion inertial fusion." DOI: 10.1103/PhysRevSTAB.8.020101 February 2005

[5] W. S. Rasband, "ImageJ," U. S. National Institutes of Health, Bethesda, Maryland, USA, http://rsb.info.nih.gov/ij/, 1997-2005

Tables

Table 1. Maximum voltage at fixed background cutoff (see text).

Image Number	Maximum Voltage (kV)
1	1.85
2	1.83
3	1.87
4	1.94
5	1.85
6	2.01
7	1.92
8	2.04

Table 2. Effect of varying background cutoff (see text).

	Background Cutoff		
Image #	90	130	200
4	1.86	1.90	1.949
5	1.783	1.817	1.855
6	1.929	1.972	2.015
7	1.839	1.878	1.920
8	1.948	1.995	2.043

Figures

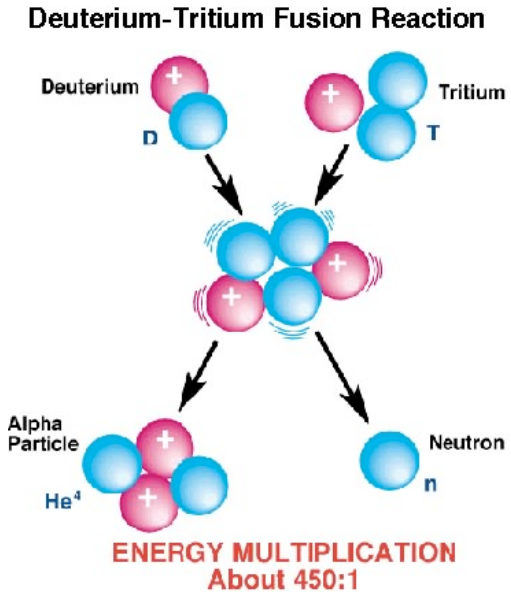

Figure 1. Schematic of "D-T" fusion reaction, from {REF. 2}.

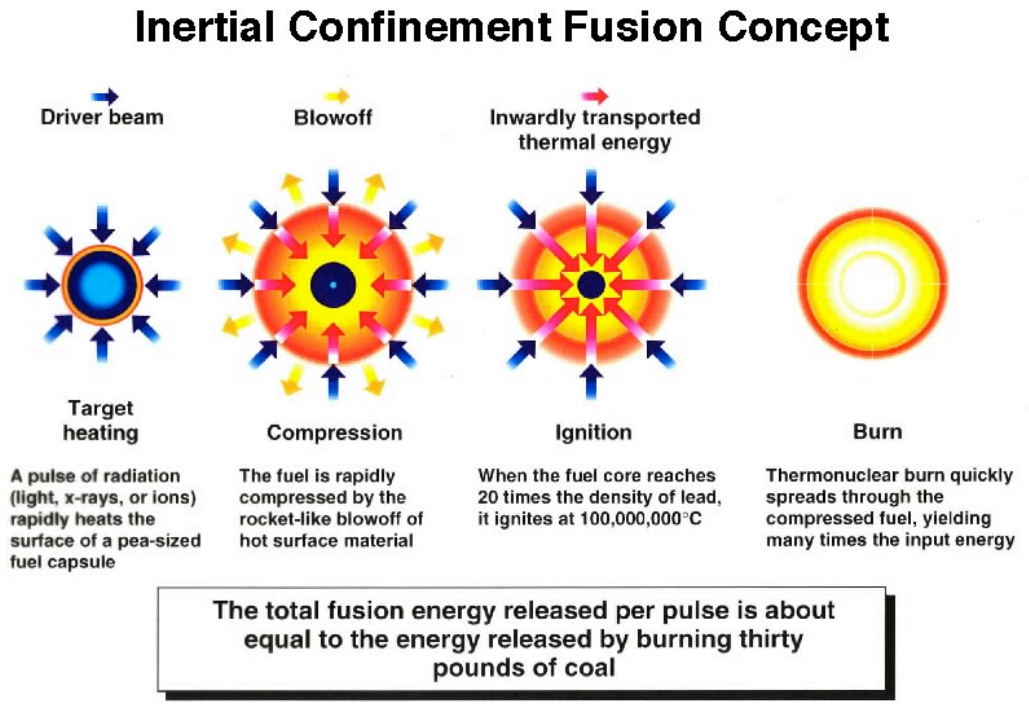

Figure 2. Demonstration of Fusion Process, from {REF. 2}

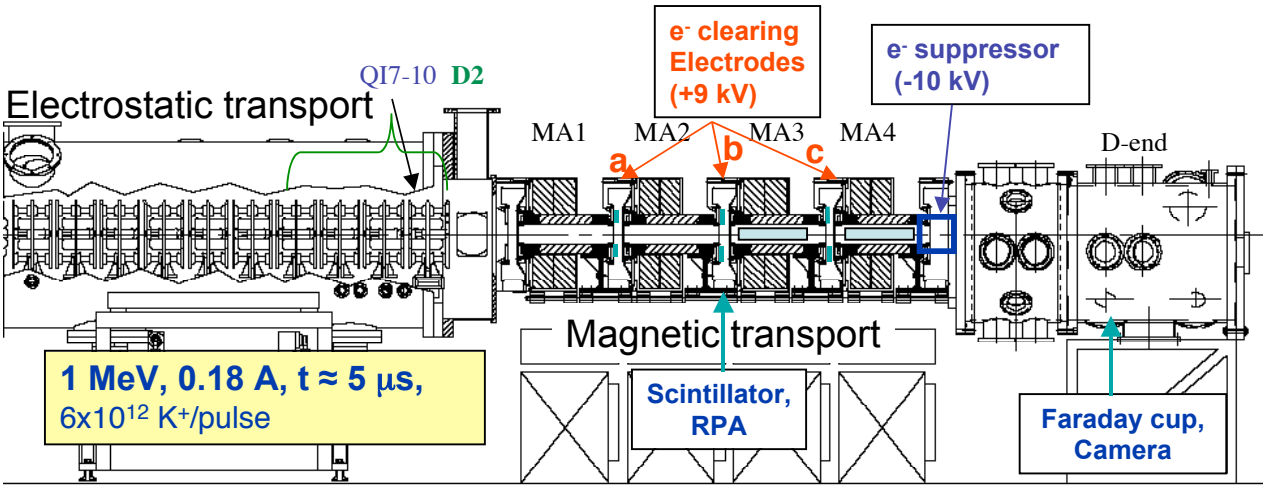

Figure 3 HCX Instrumented to carry out electron cloud experiments

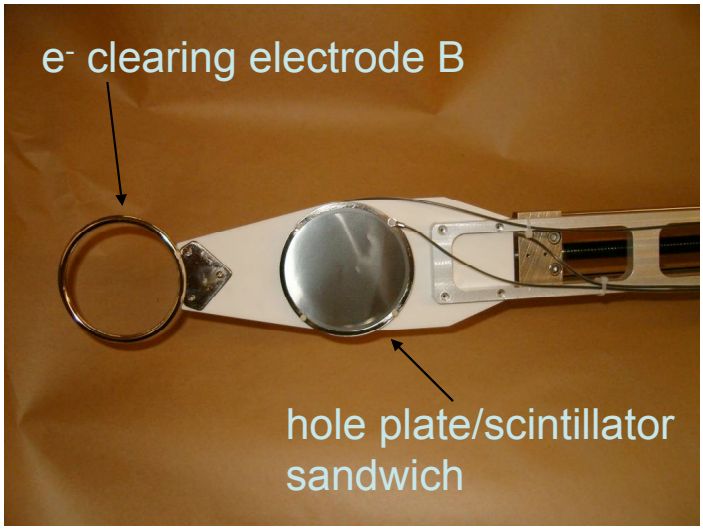

Figure 4 Scintillator

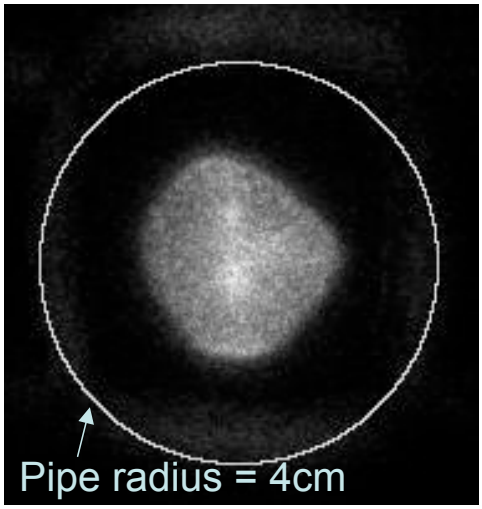

Figure 5 Scintillator Image

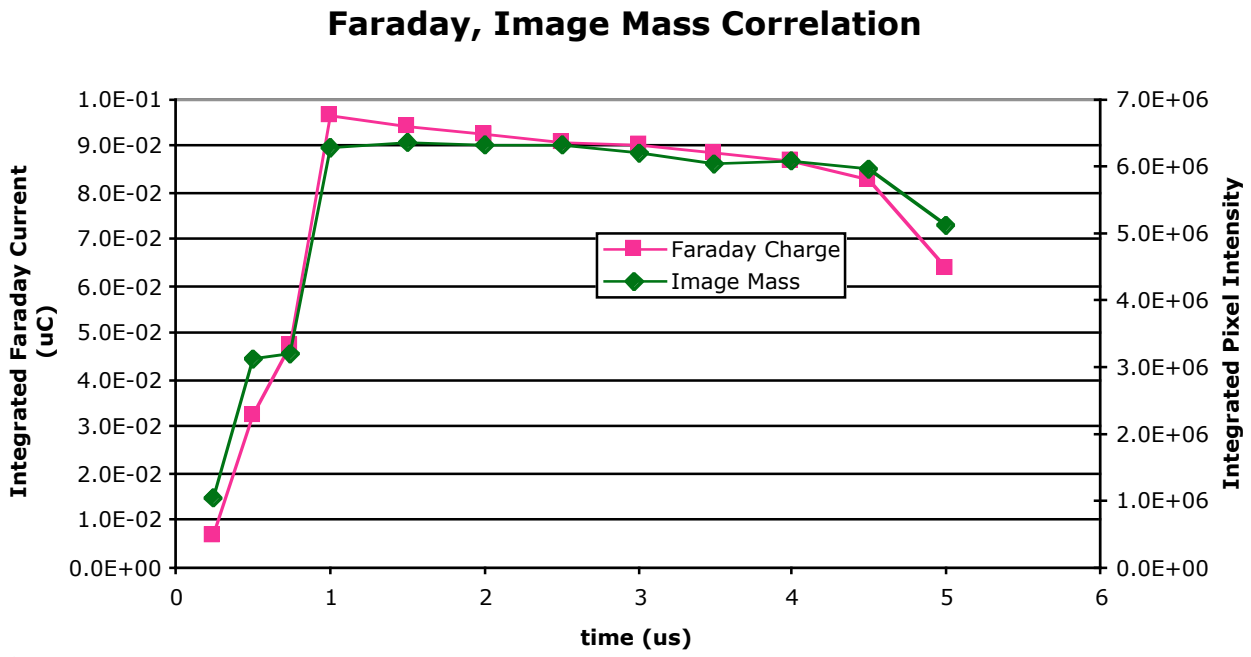

Figure 6 Shows the close correlation between Faraday data, and total image intensity over time

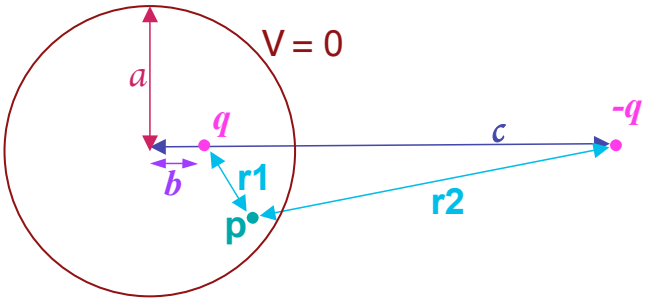

a = radius of cylinder
q = line charge
$-q$ = image charge

Equations

$$c = a^2/b$$

$$V(p) = \frac{q}{2\pi\varepsilon_o} \ln(r2/r1) - V_o$$

V_o : constant set so that $V(a)=0$

Figure 7 Diagram and equations used to calculate potentials at each point within the beam pipe.

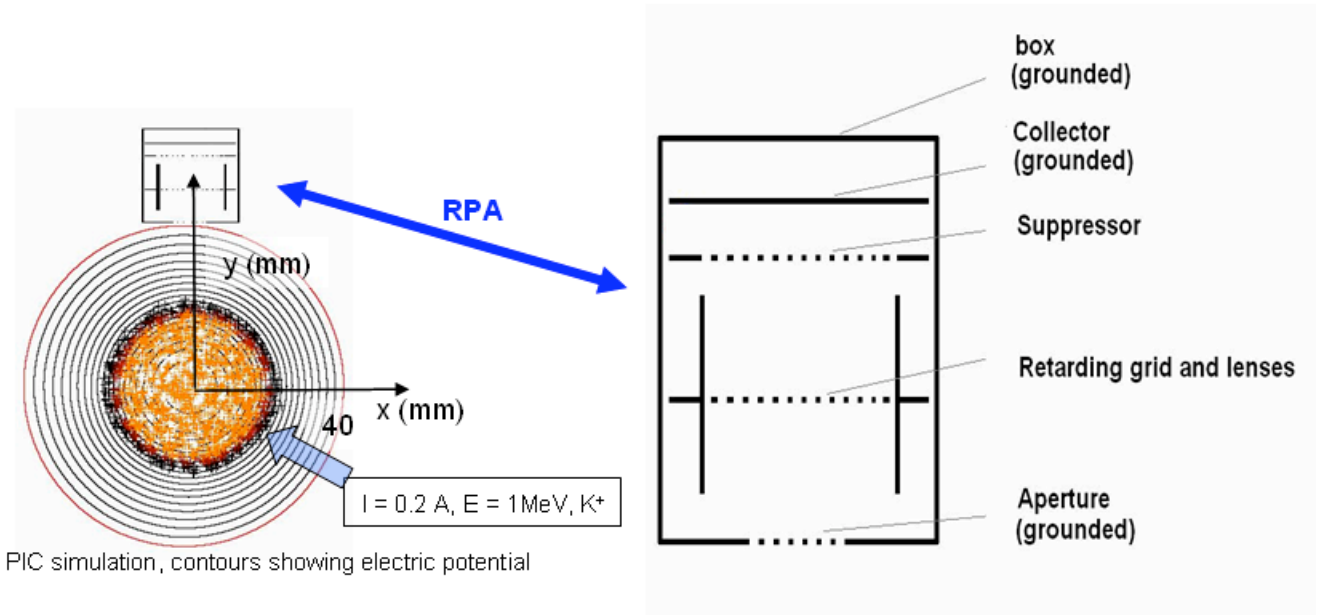

Figure 8 Shows location of Retarding Potential Analyzer (RPA), in reference to a simulated charge distribution

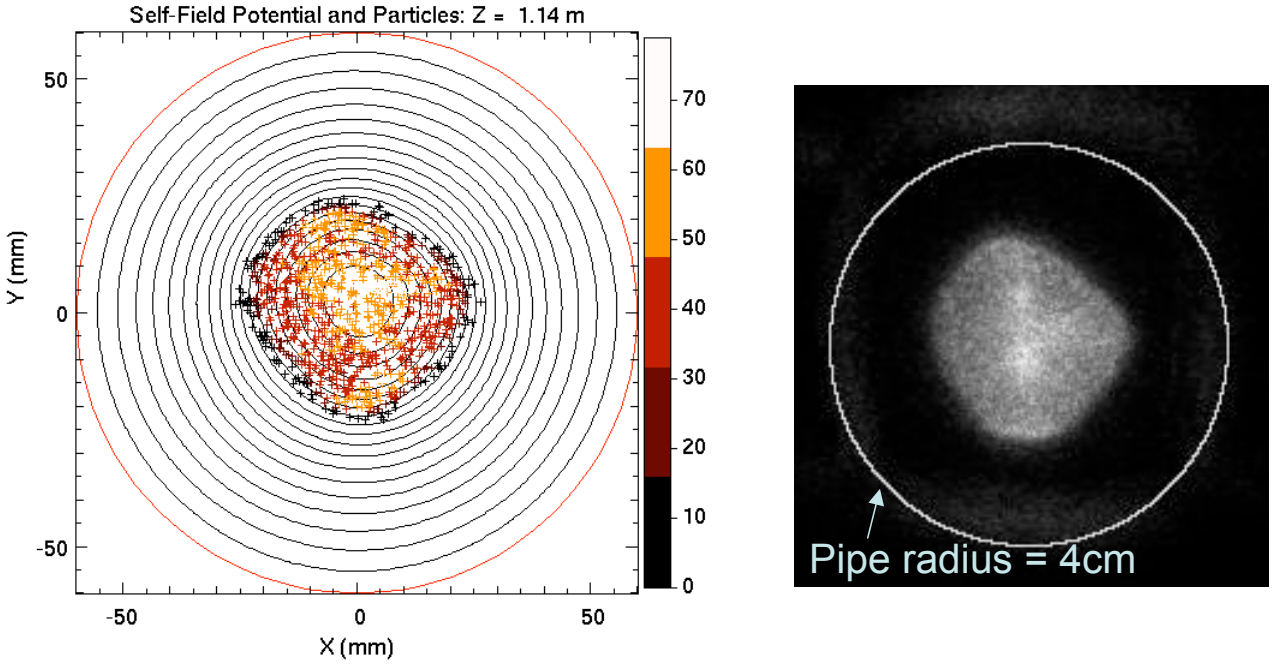

Figure 9 Comparison of simulated ion distribution at gap B initialized with “D2 data reconstruction method” with a scintillator image

Figure 10

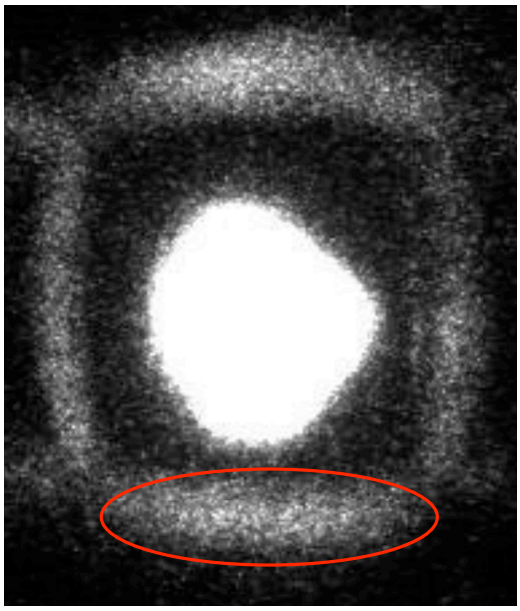

Noise, at the location of the beam pipe's narrowest dimensions, enhanced to visibility.

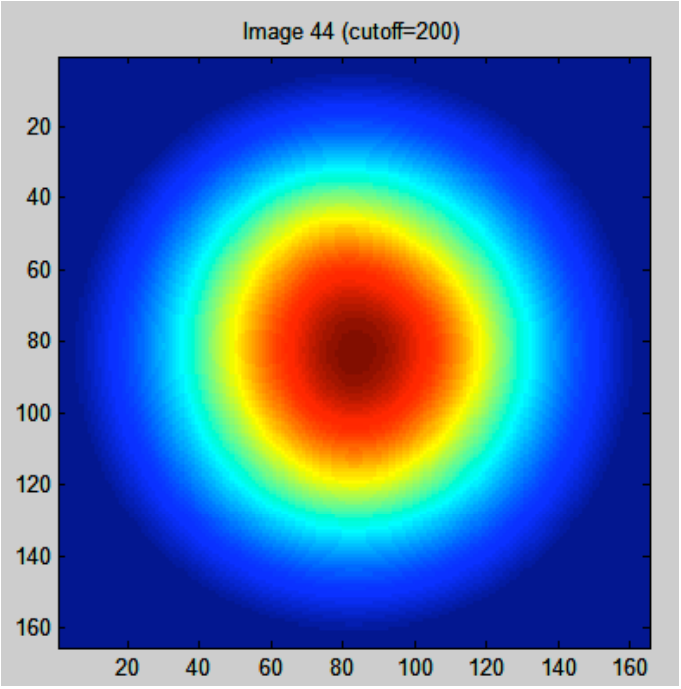

Figure 11 Representative Voltage Distribution

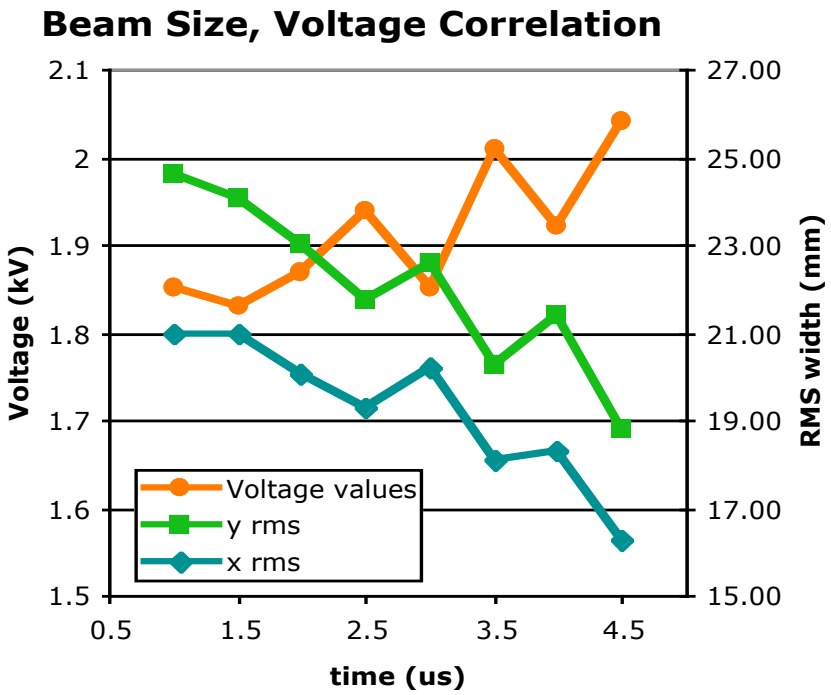

Figure 12. Shows correlation of RMS beam size with peak Voltage (kV)

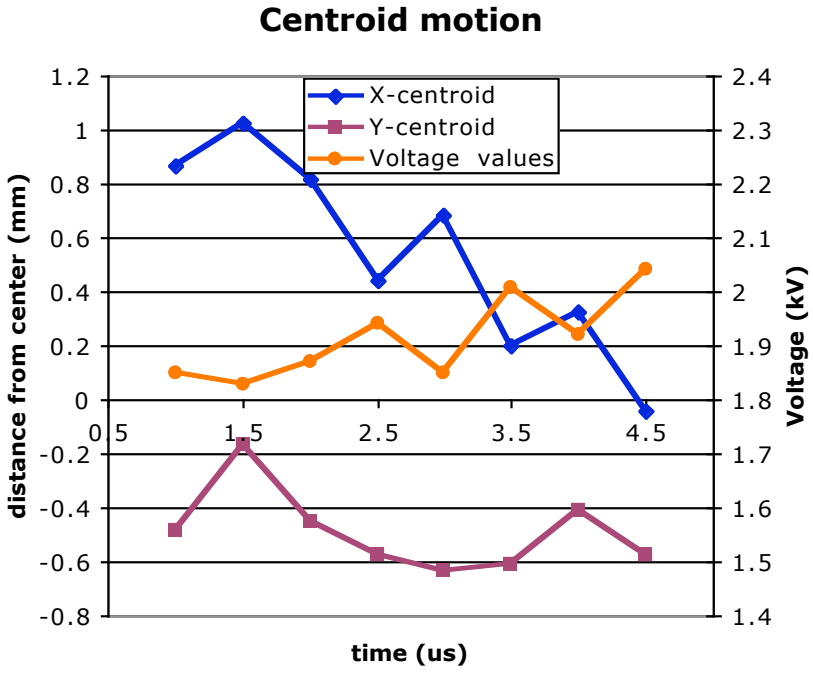

Figure 13. Shows correlation of beam centroid motion (mm) with peak voltage

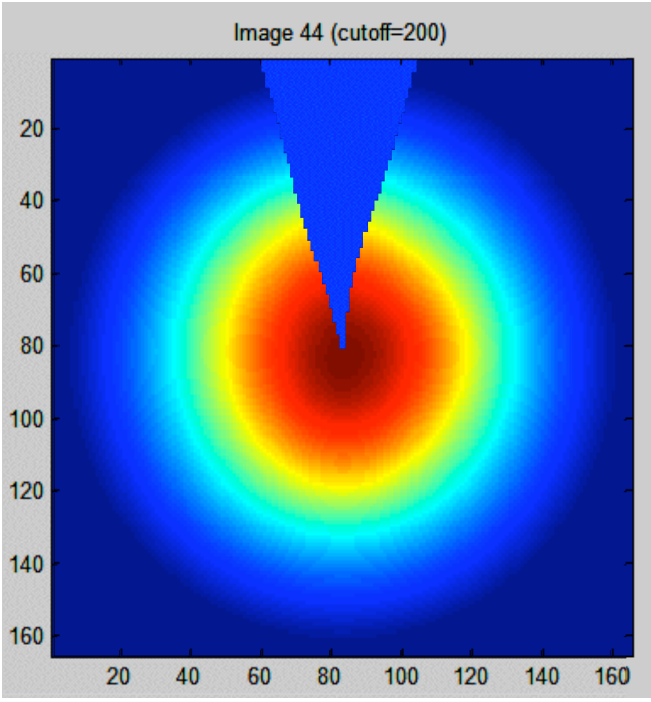

Figure 14 Blue slice represents starting positions Of particles that enter the RPA

Figure 15

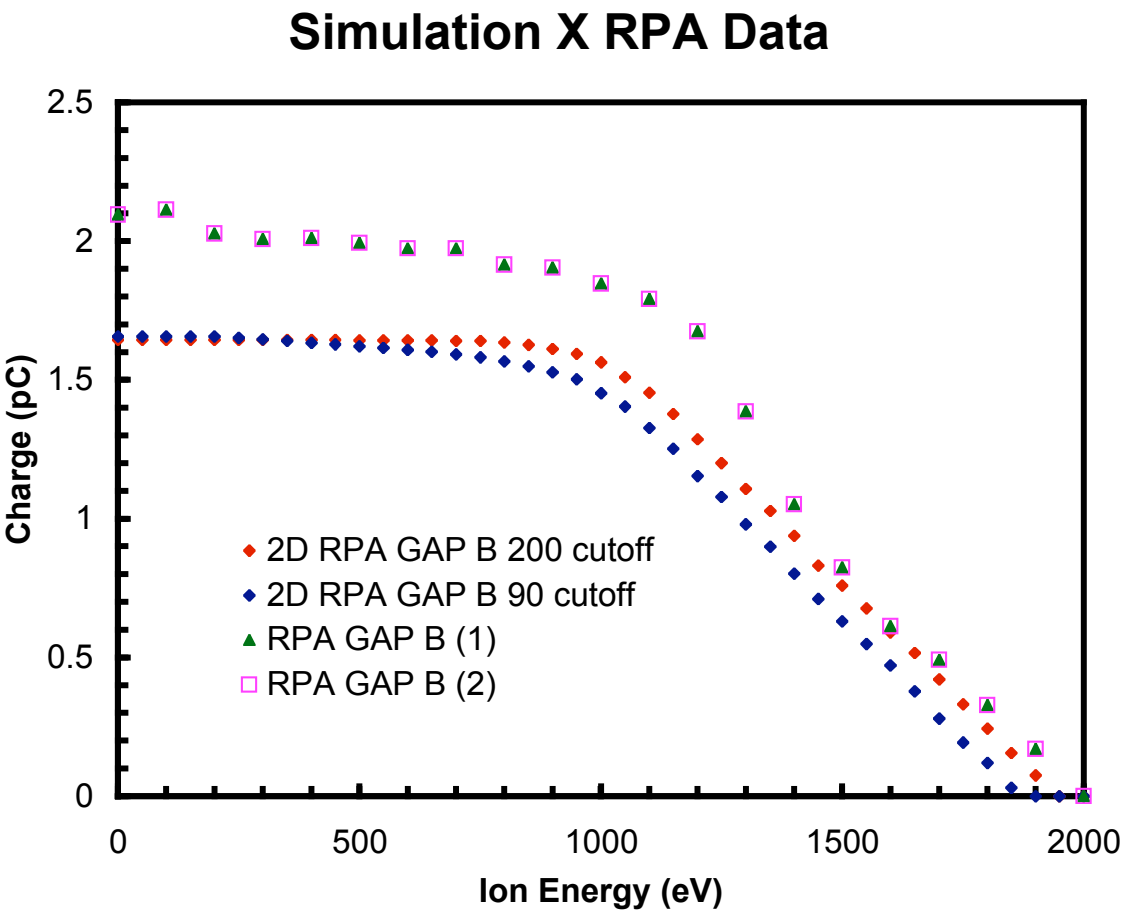

Shows the comparison of particles originating at potential steps calculated from the scintillator images, and measured with the RPA.